



# Densities, Refractive Indices, and Derived Properties of Binary Mixtures of Ethanol with Benzene and Pyridine at Various Temperatures Under Atmospheric Pressure

Fisnik Aliaj<sup>1</sup> · Naim Sylal<sup>1</sup> · Ardita Kurtishaj<sup>1</sup> · Njomza Elezaj<sup>1</sup> · Zeqë Tolaj<sup>1</sup> · Tahir Arbneshi<sup>2</sup> · Arbër Zeqiraj<sup>1,3</sup>

Received: 2 September 2019 / Accepted: 22 February 2020 / Published online: 3 March 2020  
© Springer Science+Business Media, LLC, part of Springer Nature 2020

## Abstract

Experimental densities at (293.15, 298.15, 303.15, 308.15, and 313.15) K and refractive indices at 298.15 K are reported for the binary liquid mixtures of ethanol with benzene and pyridine over the entire range of compositions and atmospheric pressure. From these experimental data, the excess molar volumes  $V^E$  and deviations in molar refractivity  $\Delta R$  were derived and fitted by the Redlich–Kister polynomial to determine the adjustable fitting parameters and the standard deviations. The number of adjustable parameters to be included in a Redlich–Kister polynomial for fitting the derived properties was optimized with the  $F$ -test.  $V^E$  values are found to be negative over the entire composition range in ethanol + pyridine mixtures, without considerable changes over the temperature range studied. In the ethanol + benzene mixtures, the  $V^E$  results show an S-shaped composition dependence, and the temperature contribution was found to be very important. The variation of  $V^E$  with composition and temperature has been interpreted in terms of molecular interactions between the components of the mixture and structural effects.  $\Delta R$  values are found to be negative for both mixtures with a minimum located between 0.45 and 0.5 volume fractions of ethanol. Furthermore, several theoretical and empirical mixing rules were applied to predict refractive indices of mixtures in order to test their validity for the present systems.

**Keywords** Excess molar volume ·  $F$ -test · Mixing rules · Molar refractivity · Redlich–Kister polynomial · Thermophysical properties

---

**Electronic supplementary material** The online version of this article (<https://doi.org/10.1007/s10765-020-02632-9>) contains supplementary material, which is available to authorized users.

---

✉ Naim Sylal  
naim.sylal@uni-pr.edu

Extended author information available on the last page of the article

## 1 Introduction

Alcohols and aromatic hydrocarbons alone or in mixtures are essential for various chemical and industrial processes [1–4]. Benzene is a non-polar aromatic hydrocarbon and the most versatile from the viewpoint of its uses. Pyridine is structurally analogous to benzene, with one methine group (=CH–) being replaced by an N atom. However, in contrast to benzene, pyridine exhibits a permanent dipole moment that is traceable to the higher electronegativity of N compared with C [5]. Ethanol is a polar liquid, strongly self-associated by H-bonded linear chains (OH···HO interactions) to the extent of polymerization that may differ depending on the temperature [6–8]. Mixing ethanol with aromatics induces dissociation of some of the H-bonded structures leading to the possibility of formation of weak  $\pi$ ···HO bonding between the  $\pi$ -electron cloud of the aromatic ring and the proton of the hydroxyl group of ethanol. Weak H-bonding of aromatic rings with proton donors (like ethanol) plays an essential role in the structure of certain biomolecules [9].

In the mixture with benzene, ethanol is widely used for the extraction of volatiles in the pulp and paper industry, and diesel exhaust particulates (see Šerbanović et al. [10] and references therein). Also, an increase in the conversion of refined coal and oil yield is achieved when raw mined coal is thermally pretreated with a binary mixture of benzene with ethanol [11]. On the other hand, a significant improvement in the coking resistance of SOFCs with Ni cermet anode operating on ethanol fuel is achieved by applying pyridine as a fuel additive [12]. Pyridine alone or in combination with other chemicals is also widely used as a denaturing additive to ethanol. Ethanol is also widely used as an additive to gasoline in order to improve fuel-combustion efficiency and reduce exhaust emissions of CO and hydrocarbons [13]. Since these substances alone or in mixtures are ubiquitous environmental pollutants, some of which exhibit cancerous features, it is of great interest to know their physical and derived properties at different temperatures and to cover the whole composition range. These properties are essential for the design and setup of separation processes and processing equipment, and they will contribute to the fundamental understanding of complex molecular interactions present in those mixtures.

Here, we present experimental densities  $\rho$  from 293.15 K to 313.15 K at 5 K intervals and refractive indices  $n$  at 298.15 K and local atmospheric pressure  $\sim 950$  hPa for the ethanol + benzene and ethanol + pyridine mixtures covering the entire mole fraction range. The related properties, excess molar volumes ( $V^E$ ), and deviations in molar refractivity ( $\Delta R$ ) were derived from experimental data. The  $V^E$  and  $\Delta R$  data were then fitted by the Redlich–Kister polynomial [14] to determine the adjustable fitting parameters and the standard deviations. The results have been interpreted in terms of molecular interactions between the components of the mixture and structural effects.

A review of published literature revealed that some thermophysical properties of the investigated mixtures had been reported [10, 13, 15–22]. For the system ethanol + benzene, Šerbanović et al. [10] and Gonzalez-Olmos et al. [13]

have reported  $\rho$  and  $V^E$  data in the temperature range covered in this work. The obtained results are in good agreement with literature values in the region of overlap. Other reports on  $\rho$  and/or  $V^E$  are available: for ethanol + benzene system at 288.15 K and 323.15 K [21], 298.15 K [15, 17, 18, 21, 23], 303.15 K [24]; for ethanol + pyridine system at 298.15 [16, 19], 308.15 K [22]. A combined study on  $\rho$  and  $n$  (and their derived properties  $V^E$  and  $\Delta R$ , respectively) at 298.15 K has also been reported for the investigated systems [15, 16]. Recently, Dikio et al. [20] have published  $\rho$  and  $V^E$  data for the ethanol + pyridine system in the temperature range from 293.15 K to 323.15 K at 10 K intervals. A detailed inspection revealed that the accuracy of the results of Dikio et al., as they compare to the published data and the results of the present study, cannot be guaranteed. Furthermore, in the present study, we used purer reagents and have investigated the influence of temperature on these systems by using apparatuses with better temperature stability than Dikio et al.

Additionally, the Lorentz–Lorenz (L–L), Eykman (EYK), Dale–Gladstone (D–G), Oster (OST), and Newton (NEW) mixing rules [25–33] were used to calculate the refractive indices of the investigated liquid mixtures. The calculated results were compared with experimental data, and the deviations are reported in terms of mean absolute percentage deviation (MAPD).

## 2 Experimental Section

### 2.1 Materials

All chemicals were obtained from Sigma-Aldrich® and were used as supplied. Table 1 shows the source and purity of the chemicals used. The mixtures were prepared by mass and were kept in airtight glass containers. Preferential evaporation during the preparation of mixtures was minimized by always charging the higher-boiling component first. The vapor space in the glass containers was reduced to a minimum in order to avoid losses by evaporation during manipulation. Mass measurements were performed in an analytic balance (KERN & Sohn GmbH, model ABS 220-4N) with precision  $\pm 0.1$  mg. Conversion from mass to molar quantities was based on the relative atomic mass Table of 2011 issued by IUPAC [34]. The overall uncertainty in the mole fraction of the studied mixtures was estimated to be within  $\pm 0.0001$ , depending on composition. Fifteen mixtures of ethanol + benzene and 18 mixtures of ethanol + pyridine were prepared to cover the whole mole fraction range. All mixtures were prepared just before use for measurements of density

**Table 1** Chemical information

Chemical name	CAS no.	Source	Purity mass fraction
Ethanol	64-17-5	Sigma-Aldrich	$\geq 0.999$
Benzene	71-43-2	Sigma-Aldrich	$\geq 0.997$
Pyridine	110-86-1	Sigma-Aldrich	$\geq 0.995$

and refractive index. Densities were studied at  $T=(293.15, 298.15, 303.15, 308.15,$  and  $313.15)$  K, and refractive indices at 298.15 K only, under a local atmospheric pressure of  $\sim 950$  hPa.

## 2.2 Apparatus and Procedures

Densities were measured as a function of temperature from 293.15 K to 313.15 K at 5 K intervals by using an Anton Paar DSA5000M digital vibrating U-tube densimeter (with automatic viscosity correction). The density measurement regime was isophletal. The repeatability of density and temperature measurements stated by the manufacturer are  $\pm 0.001$  kg·m<sup>-3</sup> and  $\pm 0.001$  K, respectively. The densimeter was calibrated periodically with Anton Paar's ultrapure water and dry air. The density and temperature standard uncertainties supplied by the manufacturer are equal to  $\pm 0.005$  kg·m<sup>-3</sup> and  $\pm 0.01$  K, respectively. The combined expanded uncertainty (with a 0.95 level of confidence) of density measurements is estimated to be better than  $\pm 0.03$  kg·m<sup>-3</sup>. Refractive indices were measured with sodium D-line by using a Schmidt + Haensch refractometer (model AR12), thermostatically controlled at  $298.15 \pm 0.04$  K. The combined expanded uncertainty (with 0.95 level of confidence) of refractive index measurements is estimated to be  $\pm 0.0002$ . Regular calibration checks of the refractometer were carried out with in-house triple distilled water to ensure the accuracy of the measurements. At least three independent measurements were performed for each composition, and the average value was considered in all calculations. Density and refractive index uncertainties were calculated using the law of propagation of uncertainty [35].

## 3 Results and Discussion

A comparison of densities and refractive indices of pure chemicals at 298.15 K to the literature data appears in Table 2. Refractive indices obtained in this work for the pure components agree with the literature values with an absolute percentage deviation (APD) of better than 0.003 %, 0.007 %, and 0.002 % for ethanol, benzene, and pyridine, respectively. The experimental densities of the pure components agree with the literature values with an APD of better than 0.004 %, 0.006 %, and 0.008 % for ethanol, benzene, and pyridine, respectively.

Tables 3 and 4 list the densities from 293.15 K to 313.15 K at 5 K intervals and refractive indices at 298.15 K, respectively, for ethanol (1)+benzene (2) and ethanol (1)+pyridine (2) mixtures against the mole fraction of ethanol,  $x_1$ . Densities and refractive indices of the investigated mixtures have been reported previously [10, 13, 15–22]. The experimental results are in agreement with the literature values. For example, the experimental densities of the ethanol + benzene system agree with the results of Šerbanović et al. [10] with an APD of better than 0.020 %, 0.021 %, 0.020 %, 0.020 %, and 0.019 % at 293.15 K, 298.15 K, 303.15 K, 308.15 K, and 313.15 K, respectively. The measured densities of ethanol + pyridine system at 298.15 K agree with the results of Findlay and Copp [19] with an APD of better than 0.021 %. Han et al. [15] reported

**Table 2** Comparison between experimental values of density  $\rho$  and refractive index  $n$  of pure components and literature values at  $T=298.15$  K and atmospheric pressure

Chemical name	$\rho/\text{kg}\cdot\text{m}^{-3}$		APD <sup>a</sup> /%	$n$		APD <sup>a</sup> /%
	This work	Literature		This work	Literature	
Ethanol	785.25	785.27 [15]	0.003	1.3593	1.35 928 [15]	0.001
		785.22 [43]	0.004		1.35 926 [43]	0.003
		785.25 [17]	0.000		1.35 933 [16]	0.002
Benzene	873.69	873.64 [44]	0.006	1.4977	1.4978 [45]	0.007
		873.68 [23]	0.001		1.49 764 [15]	0.004
		873.65 [18]	0.005			
Pyridine	978.05	978.10 [36]	0.005	1.5070	1.50 701 [36]	0.0007
		978.13 [16]	0.008		1.50 703 [16]	0.002
		987.04 [19]	0.001			

Standard uncertainties are:  $u(T)=0.01$  and  $0.04$  K for measurements of  $\rho$  and  $n$ , respectively; and the combined expanded uncertainties (with 0.95 level of confidence) are:  $U_c(\rho)=0.03$   $\text{kg}\cdot\text{m}^{-3}$  and  $U_c(n)=0.0002$

<sup>a</sup>APD (absolute percentage deviation) =  $|Y^{\text{exp}} - Y^{\text{lit}}| \cdot 100 / Y^{\text{exp}}$ ;  $Y = \rho$  or  $n$

results on densities and refractive indices for the ethanol+benzene system at 298.15 K. Our densities agree with their values with an APD of better than 0.017 %; refractive indices agree within 0.12 %. Noh et al. [16] measured densities and refractive indices of ethanol+pyridine mixtures at 298.15 K. Their experimental values agree with our own within an APD of 0.84 % and 0.11 % for the density and refractive index, respectively. Figures 1 and 2 show the percentage deviations of our measurements of densities and refractive indices from the literature for the ethanol+benzene and ethanol+pyridine systems, respectively.

From experimental densities and refractive indices of pure substances and mixtures, we have calculated excess molar volumes,  $V^E$ , and deviations in molar refractivity,  $\Delta R$ , with the following well-known equations [15, 16, 25, 36, 37]:

$$V^E = \sum_i x_i M_i (\rho^{-1} - \rho_i^{-1}), \quad (1)$$

$$\Delta R = R_m - \sum_i \phi_i R_i, \quad (2)$$

$$R_m = \left( \frac{n^2 - 1}{n^2 + 1} \right) \left( \frac{\sum_i x_i M_i}{\rho} \right), \quad (3)$$

$$R_i = \left( \frac{n_i^2 - 1}{n_i^2 + 1} \right) \left( \frac{M_i}{\rho_i} \right), \quad (4)$$

and

**Table 3** Experimental densities  $\rho$  of ethanol + (benzene or pyridine) mixtures at temperature  $T$  and local atmospheric pressure  $P \sim 950$  hPa against the mole fraction of ethanol  $x_1$ 

$T/K$	$x_1$	$\rho/\text{kg}\cdot\text{m}^{-3}$	$x_1$	$\rho/\text{kg}\cdot\text{m}^{-3}$	$x_1$	$\rho/\text{kg}\cdot\text{m}^{-3}$	$x_1$	$\rho/\text{kg}\cdot\text{m}^{-3}$
Ethanol (1) + benzene (2)								
293.15	0.0000	879.02	0.2018	865.45	0.4982	843.54	0.8491	809.14
293.15	0.0127	878.04	0.2501	862.14	0.6003	834.73	0.9000	802.97
293.15	0.0488	875.58	0.3001	858.64	0.6990	825.39	0.9509	796.37
293.15	0.0994	872.24	0.4004	851.27	0.7990	814.87	1.0000	789.54
293.15	0.1480	869.06						
298.15	0.0000	873.69	0.2018	860.16	0.4982	838.50	0.8491	804.59
298.15	0.0127	872.69	0.2501	856.88	0.6003	829.81	0.9000	798.50
298.15	0.0488	870.22	0.3001	853.42	0.6990	820.60	0.9509	791.99
298.15	0.0994	866.90	0.4004	846.14	0.7990	810.24	1.0000	785.25
298.15	0.1480	863.73						
303.15	0.0000	868.34	0.2018	854.83	0.4982	833.42	0.8491	800.00
303.15	0.0127	867.34	0.2501	851.58	0.6003	824.86	0.9000	794.00
303.15	0.0488	864.85	0.3001	848.16	0.6990	815.78	0.9509	787.59
303.15	0.0994	861.53	0.4004	840.96	0.7990	805.56	1.0000	780.94
303.15	0.1480	858.38						
308.15	0.0000	863.00	0.2018	849.47	0.4982	828.30	0.8491	795.37
308.15	0.0127	861.96	0.2501	846.25	0.6003	819.85	0.9000	789.45
308.15	0.0488	859.45	0.3001	842.85	0.6990	810.91	0.9509	783.14
308.15	0.0994	856.13	0.4004	835.74	0.7990	800.85	1.0000	776.59
308.15	0.1480	853.00						
313.15	0.0000	857.66	0.2018	844.08	0.4982	823.13	0.8491	790.69
313.15	0.0127	856.57	0.2501	840.88	0.6003	814.80	0.9000	784.87
313.15	0.0488	854.03	0.3001	837.51	0.6990	805.98	0.9509	778.66
313.15	0.0994	850.71	0.4004	830.48	0.7990	796.09	1.0000	772.20
313.15	0.1480	847.58						
Ethanol (1) + pyridine (2)								
293.15	0.0000	983.08	0.2984	940.49	0.5994	887.28	0.8491	831.05
293.15	0.0491	976.60	0.3996	924.02	0.6489	877.16	0.8916	820.00
293.15	0.1001	969.66	0.4540	914.63	0.7037	865.40	0.9275	810.31
293.15	0.1498	962.72	0.4975	906.79	0.7482	855.43	0.9681	798.91
293.15	0.2004	955.41	0.5480	897.34	0.7990	843.45	1.0000	789.54
298.15	0.0000	978.05	0.2984	935.61	0.5994	882.56	0.8491	826.55
298.15	0.0491	971.59	0.3996	919.18	0.6489	872.48	0.8916	815.56
298.15	0.1001	964.68	0.4540	909.83	0.7037	860.77	0.9275	805.91
298.15	0.1498	957.77	0.4975	902.02	0.7482	850.84	0.9681	794.57
298.15	0.2004	950.48	0.5480	892.60	0.7990	838.90	1.0000	785.25
303.15	0.0000	973.01	0.2984	930.70	0.5994	877.83	0.8491	822.03
303.15	0.0491	966.57	0.3996	914.33	0.6489	867.78	0.8916	811.09
303.15	0.1001	959.69	0.4540	905.00	0.7037	856.11	0.9275	801.49
303.15	0.1498	952.79	0.4975	897.22	0.7482	846.21	0.9681	790.21
303.15	0.2004	945.53	0.5480	887.83	0.7990	834.33	1.0000	780.94

**Table 3** (continued)

<i>T</i> /K	<i>x</i> <sub>1</sub>	<i>ρ</i> /kg·m <sup>-3</sup>	<i>x</i> <sub>1</sub>	<i>ρ</i> /kg·m <sup>-3</sup>	<i>x</i> <sub>1</sub>	<i>ρ</i> /kg·m <sup>-3</sup>	<i>x</i> <sub>1</sub>	<i>ρ</i> /kg·m <sup>-3</sup>
308.15	0.0000	967.97	0.2984	925.78	0.5994	873.06	0.8491	817.48
308.15	0.0491	961.54	0.3996	909.45	0.6489	863.05	0.8916	806.58
308.15	0.1001	954.67	0.4540	900.15	0.7037	851.41	0.9275	797.03
308.15	0.1498	947.80	0.4975	892.39	0.7482	841.56	0.9681	785.81
308.15	0.2004	940.56	0.5480	883.03	0.7990	829.72	1.0000	776.59
313.15	0.0000	962.94	0.2984	920.83	0.5994	868.26	0.8491	812.90
313.15	0.0491	956.50	0.3996	904.55	0.6489	858.29	0.8916	802.05
313.15	0.1001	949.65	0.4540	895.28	0.7037	846.69	0.9275	792.54
313.15	0.1498	942.80	0.4975	887.54	0.7482	836.88	0.9681	781.38
313.15	0.2004	935.57	0.5480	878.20	0.7990	825.09	1.0000	772.20

Standard uncertainties are: *u*(*T*)=0.01 K; *u*(*x*<sub>1</sub>)=0.0001; *u*(*P*)=10 hPa; and the combined expanded uncertainty (with 0.95 level of confidence) is *U*<sub>c</sub>(*ρ*)=0.03 kg·m<sup>-3</sup>

**Table 4** Experimental refractive indices *n* of ethanol+(benzene or pyridine) mixtures at temperature *T*=298.15 K and local atmospheric pressure *P*=~950 hPa against the mole fraction of ethanol *x*<sub>1</sub>

<i>x</i> <sub>1</sub>	<i>n</i>	<i>x</i> <sub>1</sub>	<i>n</i>	<i>x</i> <sub>1</sub>	<i>n</i>	<i>x</i> <sub>1</sub>	<i>n</i>
Ethanol (1)+ benzene (2)							
0.0000	1.4977	0.2018	1.4773	0.4982	1.4420	0.8491	1.3883
0.0127	1.4967	0.2501	1.4720	0.6003	1.4280	0.9000	1.3790
0.0488	1.4931	0.3001	1.4664	0.6990	1.4133	0.9509	1.3692
0.0994	1.4880	0.4004	1.4545	0.7990	1.3970	1.0000	1.3593
0.1480	1.4830						
Ethanol (1)+ pyridine (2)							
0.0000	1.5070	0.2984	1.4738	0.5994	1.4327	0.8491	1.3901
0.0491	1.5021	0.3996	1.4610	0.6489	1.4249	0.8916	1.3820
0.1001	1.4967	0.4540	1.4537	0.7037	1.4160	0.9275	1.3748
0.1498	1.4913	0.4975	1.4477	0.7482	1.4084	0.9681	1.3662
0.2004	1.4855	0.5480	1.4404	0.7990	1.3994	1.0000	1.3593

Standard uncertainties are: *u*(*T*)=0.04 K; *u*(*x*<sub>1</sub>)=0.0001; *u*(*P*)=10 hPa; and the combined expanded uncertainty (with 0.95 level of confidence) is *U*<sub>c</sub>(*n*)=0.0002

$$\phi_i = \left( \frac{x_i M_i \rho_i^{-1}}{\sum_j x_j M_j \rho_j^{-1}} \right). \tag{5}$$

In Eqs. 1–5, *x*<sub>*i*</sub>, *M*<sub>*i*</sub>, *ρ*<sub>*i*</sub>, *φ*<sub>*i*</sub>, *n*<sub>*i*</sub>, and *R*<sub>*i*</sub> are, respectively, the mole fraction, molar mass, density, volume fraction, refractive index, and molar refractivity of the pure component *i* in the mixture; *ρ*, *n* and *R*<sub>m</sub> are the density, refractive index, and molar refractivity of the liquid mixture.

**Fig. 1** Relative (a) refractive index deviations and (b) density deviations of literature measurements from our experimental measurements of ethanol + benzene system at 298.15 K and atmospheric pressure: Han et al. [15] (○); Tanaka and Toyama [18] (□); Grguric et al. [17] (+); Serbanovic et al. [10] (×); Goznalez-Olmos et al. [13] (\*)

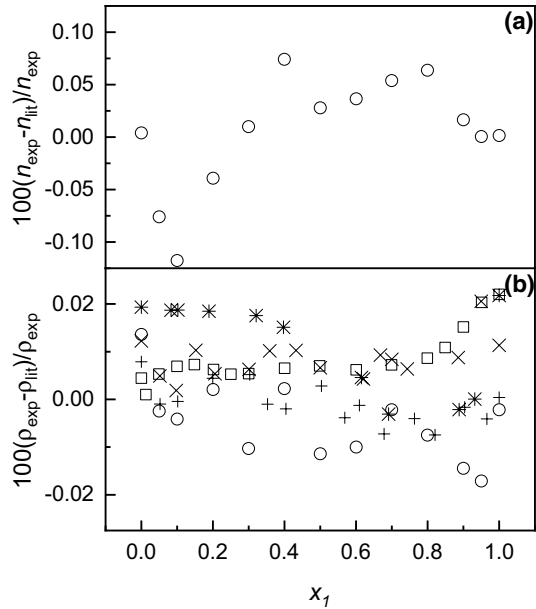
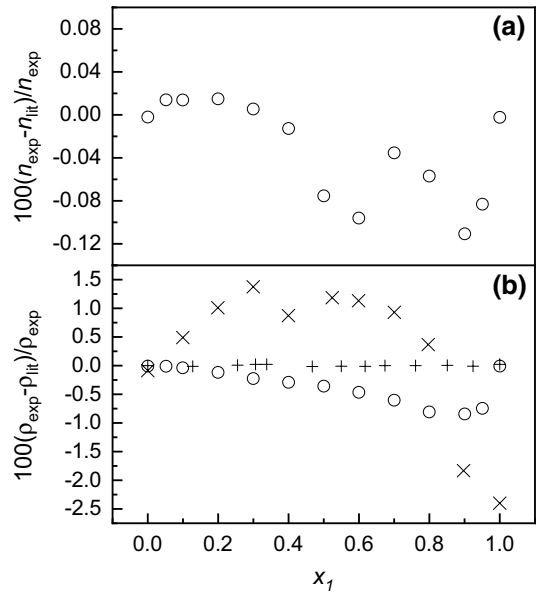


**Fig. 2** Relative (a) refractive index deviations and (b) density deviations of literature measurements from our experimental measurements of ethanol + pyridine system at 298.15 K and atmospheric pressure: Noh et al. [16] (○); Findlay and Copp [19] (+); Dikio et al. [20] (×)



The dependence of  $V^E$  on the mole fraction of ethanol  $x_1$  for the mixtures with benzene and pyridine is plotted in Figs. 3 and 4. These data are also given in Table S1, which is part of the electronic supplementary material (ESM). It was found that with increasing temperature, the  $V^E$  values only weakly increase in the ethanol + pyridine system. Thus, to avoid overcrowding of data, in Fig. 4 we have



**Fig. 3** Excess molar volumes,  $V^E$ , against the mole fraction of ethanol,  $x_1$ , for the ethanol + benzene system. Symbols refer to experimental data points at temperatures: 293.15 K ( $\square$ ); 298.15 K ( $\bullet$ ); 303.15 K ( $\nabla$ ); 308.15 K ( $\blacksquare$ ); and 313.15 K ( $\circ$ ). Solid lines are the results calculated from Eq. 6

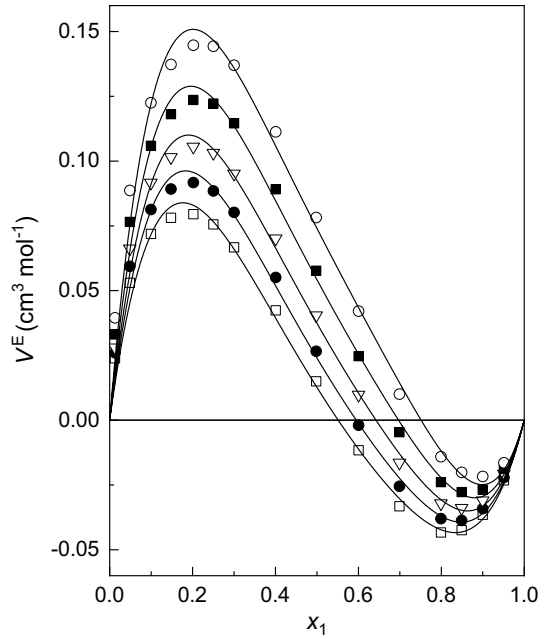
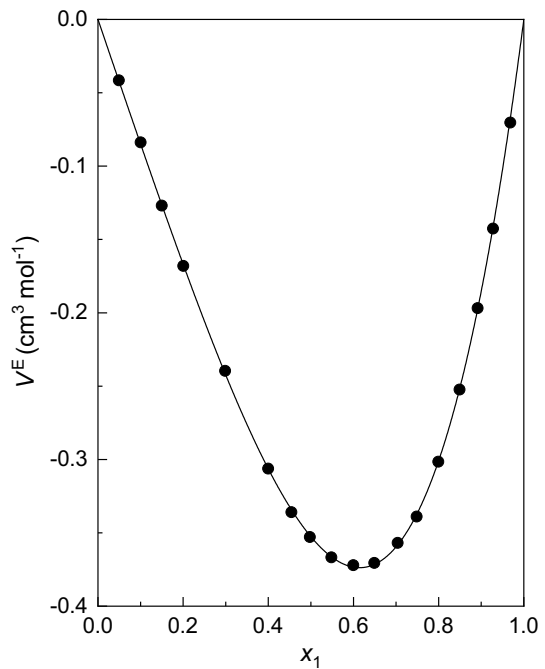


**Fig. 4** Excess molar volumes,  $V^E$ , against the mole fraction of ethanol,  $x_1$ , for the ethanol + pyridine system at 298.15 K. Solid lines are the results calculated from Eq. 6



plotted  $V^E$  against  $x_1$  at 298.15 K only. The values of  $V^E$  are negative over the entire range of compositions for the ethanol + pyridine system, whereas in the case of the ethanol + benzene system, the  $V^E$  varies much like an S-shaped curve, with positive values at lower  $x_1$  and negative values at higher  $x_1$ . Contrary to the mixtures with pyridine, the effect of temperature on  $V^E$  is noteworthy in the mixtures containing benzene, as seen in Fig. 3. There is a systematic increase in the values of  $V^E$  alongside the increase in temperature in both low- and high- $x_1$  regions. Consequently, the point on the mole fraction axis,  $x_1^0$ , where the  $V^E$  changes the sign from positive to negative values, and the equimolar  $V^E$  both increase with increasing temperature, as seen in Fig. 3 and Table 5.

The observed variations of  $V^E$  with composition can be interpreted qualitatively by considering the factors that influence this thermodynamic function. In general, the magnitude and sign of  $V^E$  depend upon several opposing contributions arising from physical, chemical, and structural factors [6, 7, 10]. The physical contributions consist mainly of dispersion forces or weak dipole–dipole interactions, resulting in positive  $V^E$  values. The chemical contributions include: (i) specific interactions such as hydrogen bonding, the formation of charge-transfer complexes, and the strong dipole–dipole interactions between the component molecules in the mixture—all leading to negative  $V^E$  values, and (ii) the stretching and breaking of molecular associates present in the pure liquids, leading to an expansion in volume and a positive contribution to  $V^E$ . The structural contribution includes the geometrical interstitial accommodation of molecules in each other's structure due to differences in the size and shape of the component molecules of the mixtures, resulting in negative  $V^E$  values.

The positive trend in  $V^E$  for the mixtures with benzene suggests that there are no strong specific interactions between components of the mixtures and that the values are a consequence of mainly the rupture of the hydrogen-bonded ethanol structures as the ethanol molecules were added to a large amount of benzene. The negative  $V^E$  values in the ethanol-rich region ( $x_1 > 0.5949$  at 298.15 K; see Table 5) indicate that complex formation occurred through  $\pi \cdots \text{HO}$  bonding between the  $\pi$ -electron cloud of the aromatic ring of benzene and the proton of the hydroxyl group of ethanol. A further negative contribution may arise from the interstitial accommodation of benzene molecules in the remaining hydrogen-bonded ethanol structure. In addition to these effects, the dispersion forces were also expected to operate between unlike molecules.

**Table 5** Values of  $x_1^0$  (the point on the mole fraction axis where the  $V^E$  changes the sign from positive to negative values) and the equimolar  $V^E$  at each investigated temperature  $T$  for the ethanol + benzene system

T/K	$x_1^0$	$V^E(x_1=0.5)/\text{cm}^3 \cdot \text{mol}^{-1}$
293.15	0.5513	0.0127
298.15	0.5949	0.0240
303.15	0.6425	0.0374
308.15	0.6969	0.0542
313.15	0.7513	0.0740

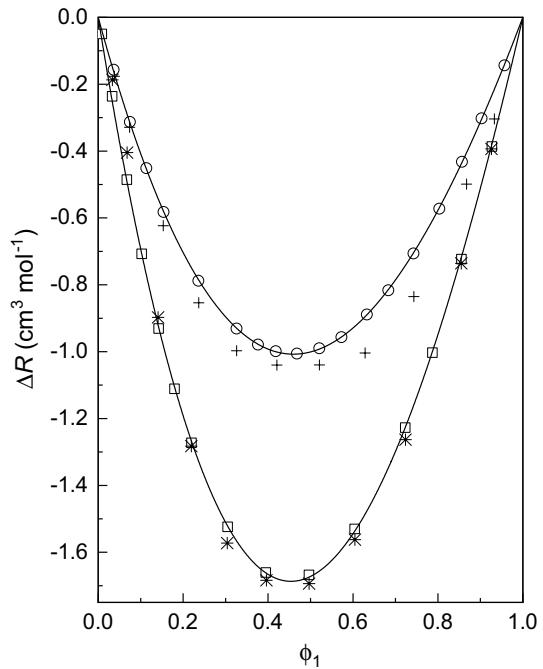
The fact that the  $V^E$  values are negative over the entire composition range in the ethanol + pyridine system suggests that the stretching and rupture of associates present in the pure liquids did not result in considerable positive  $V^E$  values. The negative deviations in  $V^E$  can be attributed mainly to the formation of complexes by strong cross-associated  $N\cdots HO$  interactions between the free lone electron pair of electronegative N-atom of pyridine and the proton of the hydroxyl group of ethanol. Additional negative contributions to  $V^E$  arise from structural effects and  $\pi\cdots HO$  bond formation between the ethanol molecules and delocalized  $\pi$ -electrons of the aromatic ring of pyridine. Kijevčanin et al. [38] have also suggested that the resulting structure and properties of mixtures of pyridine with 1-propanol and 1- and 2-propanediol are determined entirely by interactions through the  $-OH$  group and structural effects. Similar results are also obtained by Ali et al. [7] for binary mixtures of pyridine and 1-alkanols ( $C_6-C_{10}$ ).

A comparison between  $V_{min}^E$  values at each temperature of the investigated mixtures revealed that the  $V_{min}^E$  values of the mixtures with pyridine are from 8 to 15 times higher than the corresponding values in the ethanol-rich region of the mixtures with benzene, which is attributed entirely to the stronger cross-associated  $N\cdots HO$  interactions existing only in the mixtures with pyridine, forming a more compact packing than in mixtures with benzene, thus giving more negative values of  $V^E$ .

In liquid mixtures, there is always a competition between molecular interactions and disordered thermal movement of molecules. Increasing the thermal movement of molecules with increasing temperature will lead to a decrease in molecular interactions, which, as a consequence, will give rise to volume expansion. This explains the systematic increase of  $V^E$  values with the rising temperature in the ethanol + benzene mixtures. In the lower ethanol concentration region, the elevation of temperature increases the stretching and rupturing of hydrogen bonds, which results in the weakening of molecular association, thus leading to higher positive values of  $V^E$ . In the higher ethanol concentration region, the number of cross-associated complexes through  $\pi\cdots HO$  bonding decreases with the increasing temperature and leads to less negative  $V^E$  values. The effect of temperature on the  $V^E$  values is minimal for the mixture with pyridine. We assume that the increased thermal agitation has enabled a more compact packing of component molecules into one another's structure facilitated by  $N\cdots HO$  interactions, resulting in only slight variations in  $V^E$ . Similar results were obtained by Kijevčanin et al. [38] for the binary mixtures of pyridine with mono- and poly-alcohols.

The deviations in molar refractivity  $\Delta R$  of the studied mixtures are shown in Fig. 5 against the volume fraction of ethanol,  $\phi_1$ , and also listed in Table S2 of the ESM. The  $\Delta R$  values of both systems were found to be negative over the entire range of the compositions. We can observe that the  $\Delta R$  data exhibit a parabolic-like dependence with a minimum value located between 0.45 and 0.5 volume fractions of ethanol,  $\phi_1$ . Molar refraction deviation  $\Delta R$  represents the electronic perturbation due to orbital mixing of the components of the mixtures. Therefore,  $\Delta R$  can be used as a measure of the strength of the interaction between the components of the mixture and is strongly dependent on composition and temperature [16, 39]. Negative values of  $\Delta R$  indicate greater dispersive forces in the mixtures than pure components [40].

**Fig. 5** Deviations in the molar refractivity,  $\Delta R$ , against the volume fraction of ethanol,  $\phi_1$ , of the present work and those available in the literature at 298.15 K and atmospheric pressure. Ethanol + pyridine: this work (○); Noh et al. [16] (+); ethanol + benzene: this work (□); Han et al. [15] (\*). Solid lines are the results calculated from Eq. 6



The  $V^E$  and  $\Delta R$  data were also fitted by the unweighted least-square method to the Redlich–Kister (R–K) polynomial expression [14]:

$$Y = X(1 - X) \sum_{j=1}^k B_j(1 - 2X)^{j-1}, \quad (6)$$

which is one of the most popular expressions for the mathematical representation of excess physical or thermochemical properties of binary liquid mixtures [41]. In Eq. 6,  $X = x_1$  (mole fraction of ethanol) for  $Y = V^E$ , and  $X = \phi_1$  (volume fraction of ethanol) for  $Y = \Delta R$ ; and  $k$  is the number of adjustable fitting parameters,  $B_j$ .

The R–K power series expansion has a valuable feature that the values of the parameters of expansion are less correlated, i.e., will not vary considerably upon the total number of terms used, than the parameters of a simple power series expansion. This is an important feature because if any physical meaning is to be assigned to one of its parameters, then its value is practically constant for various orders of fit. Effectively, terms may be truncated from an R–K polynomial expansion in order to yield acceptable approximations. In this work, the number  $k$  in the R–K power series expansion, Eq. 6, was optimized by using the  $F$ -test at 0.005 significance level [42]. The  $F$ -test is a simple and robust statistical test to optimize the number of parameters to be included in the R–K polynomials for fitting thermodynamic excess and deviation properties. In general, the number of adjustable fitting parameters depends on factors such as (i) the dependence of the excess or deviation property with composition, i.e., the shape of data across the graph; (ii) the number of data points; (iii)

**Table 6** Fitted parameters  $B_j$  ( $j=1$  to  $k$ ) and standard deviations  $\sigma$  for representation with Redlich–Kister polynomial, Eq. 6, of property  $Y$  for ethanol + (benzene or pyridine) mixtures at temperature  $T$  and local atmospheric pressure  $P = \sim 950$  hPa

Property $Y^a$	$T/K$	$B_1$	$B_2$	$B_3$	$B_4$	$\sigma(Y)^b$
Ethanol + benzene						
$V^E$	293.15	0.051	0.511	0.213	0.395	0.004
	298.15	0.096	0.536	0.243	0.432	0.004
	303.15	0.150	0.564	0.271	0.467	0.005
	308.15	0.217	0.595	0.322	0.533	0.006
	313.15	0.296	0.625	0.383	0.619	0.007
$\Delta R$	298.15	-6.689	-1.263			0.007
Ethanol + pyridine						
$V^E$	293.15	-1.409	0.709	-0.146		0.001
	298.15	-1.411	0.698	-0.141		0.001
	303.15	-1.411	0.687	-0.137		0.001
	308.15	-1.407	0.683	-0.125		0.001
	313.15	-1.400	0.683	-0.109		0.001
$\Delta R$	298.15	-4.003	-0.658			0.002

Standard uncertainties are:  $u(T)=0.01$  and  $0.04$  K for  $V^E$  and  $\Delta R$ , respectively;  $u(P)=10$  hPa; and the combined expanded uncertainties (with 0.95 level of confidence) are:  $U_c(V^E)=0.009$   $\text{cm}^3\cdot\text{mol}^{-1}$  and  $U_c(\Delta R)=0.010$   $\text{cm}^3\cdot\text{mol}^{-1}$

<sup>a</sup> $Y = V^E$ , units:  $\text{cm}^3\cdot\text{mol}^{-1}$ ;  $Y = \Delta R$ , units:  $\text{cm}^3\cdot\text{mol}^{-1}$

$${}^b\sigma(Y) = \left\{ \frac{1}{N-k} \sum_{i=1}^N [Y_i^{\text{exp}} - Y_i^{\text{cal}}]^2 \right\}^{1/2}$$

the quality of the experimental data; and (iv) the level of significance. In this work, only two parameters were needed to fit the  $\Delta R$  data significantly because they exhibited a nearly symmetric parabolic dependence. Since  $V^E$  data were less symmetrical, more parameters were needed to fit those data significantly.

The values of adjustable fitting parameters,  $B_j$ , at each temperature, and the corresponding standard deviations for the  $V^E$  and  $\Delta R$  data are summarized in Table 6. The solid lines in Figs. 3, 4, 5 refer to the values calculated from Eq. 6 using the corresponding parameters  $B_j$  given in Table 6. We can observe that there is a good agreement between the experimental data and the solid lines calculated with the adjustable parameters.

Additionally, the results for refractive indices obtained by the Lorentz–Lorenz (L–L), Eykman (EYK), Dale–Gladstone (D–G), Oster (OST), and Newton (NEW) mixing rules [25–33] for the present systems are summarized in Table S3 of ESM. These mixing rules are based on the electromagnetic theory of light, which treats the molecules as dipoles or assemblies of dipoles in an external field [31]. The ability of these rules to predict the refractive indices of the investigated systems was tested by calculating the mean absolute percentage deviation (MAPD) of the predicted values from experimental ones. The MAPD results are presented in Table 7. From a perusal of Table 7, it is obvious that all the considered mixing rules performed well for both systems. The EYK rule resulted in the lowest deviation for the ethanol + benzene system. For the ethanol + pyridine system, the NEW rule shows the best agreement with experimental values, whereas the highest deviation was obtained with the L–L

**Table 7** Mean absolute percentage deviation (MAPD) for the Lorentz–Lorenz (L–L), Eykman (EYK), Oster (OST), Dale–Gladstone (D–G), and Newton (NEW) mixing rules for binary liquid mixtures of ethanol + benzene and ethanol + pyridine at 298.15 K

System	L–L	EYK	OST	D–G	NEW
Ethanol + benzene	0.024	0.020	0.071	0.038	0.096
Ethanol + pyridine	0.190	0.134	0.063	0.109	0.029

$$\text{MAPD} = \frac{100}{N} \sum_i^N \left| \frac{n_i^{\text{exp}} - n_i^{\text{cal}}}{n_i^{\text{exp}}} \right|$$

mixing rule. The observed deviations are expected and can be accounted for, to some degree, if the excess volume is taken into consideration in the various mixing rules [31]. Based on MAPD data, the predicting ability of the mixing rules follows this sequence: EYK > L–L > D–G > OST > NEW for ethanol + benzene system; NEW > OST > D–G > EYK > L–L for ethanol + pyridine system.

A comparison has also been made between our derived data ( $V^E$  and  $\Delta R$ ) and those available in the literature for the investigated mixtures, which is graphically represented in Figs. 5, 6, 7. From Fig. 5, it can be seen that the  $\Delta R$  data of this work agree well with those reported by Han et al. [15] for the ethanol + benzene mixtures. The data of Noh et al. [16] present less agreement with our own, especially at the high-volume fraction region of ethanol. We can observe that the  $V^E$  data of this work for the ethanol + benzene agree well with those reported by Šerbanović et al. [10]

**Fig. 6** Excess molar volumes,  $V^E$ , against the mole fraction of ethanol,  $x_1$ , for the ethanol + benzene system of the present work and those available in the literature: this work at 298.15 K (●) and 308.15 K (■); Šerbanović et al. [10] at 298.15 K (○) and 308.15 K (□); Han et al. [15] (\*); Gonzales-Olmos et al. [13] at 298.15 K (×); Albright et al. [23] at 298.15 K (Δ); Tanaka and Toyama [18] at 298.15 K (☆). Solid lines are the results calculated from Eq. 6

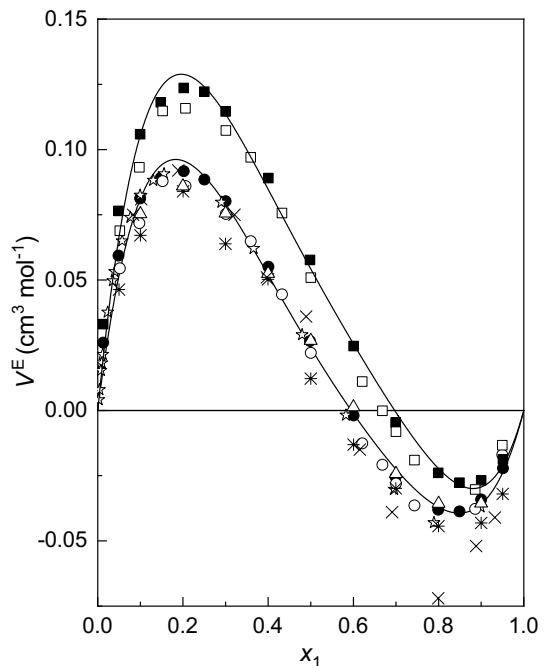
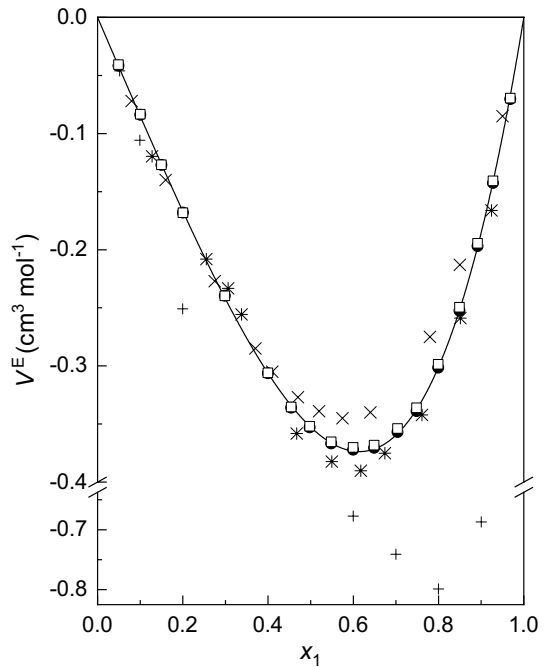


**Fig. 7** Excess molar volumes,  $V^E$ , against the mole fraction of ethanol,  $x_1$ , for the ethanol + pyridine system of the present work and those available in the literature: this work at 298.15 K (●) and 308.15 K (□); Noh et al. [16] at 298.15 K (+); Singh et al. [22] at 308.15 K (×); Findlay and Copp [19] at 298.15 K (\*). Solid lines are the results calculated from Eq. 6



at both temperatures, 298.15 K and 308.15 K, over the entire composition range, although our data are less scattered. The data of Han et al. present less agreement with our own, especially at the low mole fraction region of ethanol. We can observe that there is a large discrepancy between the  $V^E$  of Noh et al. and the results of this work for the ethanol + pyridine system, although we used liquids with similar purity and apparatus that yield results with same precision and accuracy. We believe that the accuracy of the results of Noh et al. as they compare to our results and the literature cannot be guaranteed. The data of Findlay and Coop [19] and Singh et al. [22] show good agreement with some differences observed in the mid-ethanol concentration region. The equipment used by Findlay and Coop and Singh et al. gives results with less precision and accuracy, one reason that can explain these differences.

## 4 Conclusions

This paper reports experimental data for density,  $\rho$ , and refractive index,  $n$ , for ethanol + benzene and ethanol + pyridine mixtures over the entire composition range at five temperatures  $T=(293.15, 298.15, 303.15, 308.15, \text{ and } 313.15)$  K and atmospheric pressure. From these data, excess molar volumes  $V^E$  and deviations in molar refractivity  $\Delta R$  were derived and fitted to the Redlich–Kister polynomial. Good agreement was achieved between experimental  $V^E$  and  $\Delta R$  and the results calculated by Redlich–Kister polynomial.

The values of  $V^E$  are negative over the entire composition range in ethanol + pyridine mixtures, without considerable changes over the temperature range studied. In contrast, with ethanol + benzene mixtures, the  $V^E$  results exhibited an S-shaped composition dependence, and the temperature contribution was found to be very important. This kind of behavior could be interpreted in terms of various balancing contributions arising from physical, chemical, and structural effects. The  $\Delta R$  values are negative for both mixtures with a minimum located between 0.45 and 0.5 volume fractions of ethanol.

The application of various theoretical and empirical mixing rules in predicting the refractive indices of the investigated systems showed that all of the considered mixing rules worked well for both systems. For the ethanol + benzene system, the refractive indices provided by the EYK mixing rule were closest to the experimental values. The NEW mixing rule showed the best agreement with experimental values for the ethanol + pyridine system.

## References

1. H.-G. Franck, J.W. Stadelhofer, *Industrial Aromatic Chemistry* (Springer, Berlin, 1988), pp. 132–235
2. S. Shimizu, N. Watanabe, T. Kataoka, T. Shoji, N. Abe, S. Morishita, H. Ichimura, in *Ullmann's Encyclopedia of Industrial Chemistry*, vol. 30, ed. by B. Elvers, S. Hawkins, G. Schulz (Wiley, Weinheim, 2012), p. 557
3. Y. Sekine, K. Urasaki, S. Asai, M. Matsukata, E. Kikuchi, S. Kado, *Chem. Commun.* (2005). <https://doi.org/10.1039/B412552E>
4. B.A. Raich, H.C. Foley, *Ind. Eng. Chem. Res.* **37**, 3888 (1998)
5. J.A. Joule, K. Mills, *Heterocyclic Chemistry*, 5th edn. (Wiley-Blackwell, West Sussex, 2010), pp. 5–18
6. G.P. Dubey, M. Sharma, N. Dubey, *J. Chem. Thermodyn.* **40**, 309 (2008)
7. A. Ali, M. Tariq, F. Nabi, Shahjahan. *Chinese J. Chem.* **26**, 2009 (2008)
8. S. Thirumaran, D. Priya, *Indian J. Pure Appl. Phys.* **51**, 413 (2013)
9. A. Ali, A.K. Nain, B. Lal, D. Chand, *Int. J. Thermophys.* **25**, 1835 (2004)
10. S.P. Šerbanović, M.L. Kijevčanin, I.R. Radović, B.D. Djordjević, *Fluid Phase Equilib.* **239**, 69 (2006)
11. R. N. Miller, US patent no. 4617105, 1986
12. W. Wang, F. Wang, R. Ran, H.J. Park, D.W. Jung, Ch. Kwak, Z. Shao, *J. Power Sources* **265**, 20 (2014)
13. R. Gonzalez-Olmos, M. Iglesias, S. Mattedi, *Phys. Chem. Liq.* **48**, 337 (2010)
14. O. Redlich, A.T. Kister, *Ind. Eng. Chem.* **40**, 345 (1948)
15. K.-J. Han, J.-H. Oh, S.-J. Park, *J. Ind. Eng. Chem.* **13**, 360 (2007)
16. H.-J. Noh, S.-J. Park, S.-J. In, *J. Ind. Eng. Chem.* **16**, 200 (2010)
17. I.R. Grgurić, S.P. Šerbanović, M.L. Kijevčanin, A.Ž. Tasić, B.D. Djordjević, *Thermochim. Acta* **412**, 25 (2004)
18. R. Tanaka, S. Toyama, *J. Chem. Eng. Data* **42**, 871 (1997)
19. T.J.V. Findlay, J.L. Copp, *Trans. Faraday Soc.* **65**, 1463 (1969)
20. E.D. Dikio, S.M. Nelana, D.A. Isabirye, E.E. Ebenso, *Int. J. Electrochem. Sci.* **7**, 11101 (2012)
21. K.N. Marsh, C. Burfitt, *J. Chem. Thermodyn.* **7**, 955 (1975)
22. P.P. Singh, B.R. Sharma, P.C. Chopra, *J. Chem. Thermodyn.* **12**, 1193 (1980)
23. J.G. Albright, A.V.J. Edge, R. Mills, *J. Chem. Soc. Faraday Trans.* **79**, 1327 (1983)
24. R.S. Myers, H.L. Clever, *J. Chem. Thermodyn.* **6**, 949 (1974)
25. F. Alijaj, N. Sylja, A. Bytyqi-Damoni, *AKTET J. Inst. Alb-Shkenca* **9**, 36 (2016)
26. F. Alijaj, A. Bytyqi-Damoni, N. Sylja, in *AIP Conf. Proc.* 1722, ed. by B. Akkuş, Y. Öktem, L. Ş. Yalçın, R. B. Ç. Mutlu, G. S. Doğan (AIP Publishing, 2016), p. 290015-1



27. H.A. Lorentz, *The Theory of Electrons and Its Applications to the Phenomena of Light and Radiant Heat*, 2nd edn. (B. G. Teubner, Leipzig, 1916)
28. G. Oster, *Chem. Rev.* **43**, 319 (1948)
29. W. Heller, *J. Phys. Chem.* **69**, 1123 (1965)
30. W. Heller, *Phys. Rev.* **68**, 5 (1945)
31. R. Mehra, *J. Chem. Sci.* **115**, 147 (2003)
32. A.Ž. Tasić, B.D. Djordjević, D.K. Grozdanić, N. Radojković, *J. Chem. Eng. Data* **37**, 310 (1992)
33. J.F. Eykman, *Recl. Trav. Chim. Pays-Bas* **14**, 185 (1895)
34. M.E. Wieser et al., *Pure Appl. Chem.* **85**, 1047 (2013)
35. B. N. Taylor, C. E. Kuyatt, *Guidelines for Evaluating and Expressing the Uncertainty of NIST Measurement Results (NIST Technical Note 1297, 1994 Edition)*. <http://physics.nist.gov/TN1297>. Accessed 16 Feb 2020
36. M.S. Bakshi, G. Kaur, *J. Chem. Eng. Data* **42**, 298 (1997)
37. Y.-W. Sheu, C.-H. Tu, *J. Chem. Eng. Data* **51**, 1634 (2006)
38. M.L. Kijevčanin, E.M. Živković, B.D. Djordjević, I.R. Radović, J. Jovanović, S.P. Šerbanović, *J. Chem. Thermodyn.* **56**, 49 (2013)
39. S. Singh, S. Parveen, D. Shukla, M. Gupta, J.P. Shukla, *Acta Phys. Pol. A* **111**, 847 (2007)
40. V. Aniya, A. Kumari, R. Reddy, B. Satyavathi, *J. Solut. Chem.* **46**, 1177 (2017)
41. W.E. Acree Jr., *Thermodynamic Properties of Nonelectrolyte Solutions* (Academic Press Inc., Orlando, 1984), pp. 62–73
42. P.R. Bevington, D.K. Robinson, *Data Reduction and Error Analysis for the Physical Sciences*, 3rd edn. (McGraw-Hill, New York, 2003), pp. 194–217
43. M. Tjahjono, M. Garland, *J. Solut. Chem.* **36**, 221 (2007)
44. Y. Miyano, W. Hayduk, *J. Chem. Eng. Data* **38**, 277 (1993)
45. A.Ž. Tasić, D.K. Grozdanić, B.D. Djordjević, S.P. Serbanović, N. Radojković, *J. Chem. Eng. Data* **40**, 586 (1995)

**Publisher's Note** Springer Nature remains neutral with regard to jurisdictional claims in published maps and institutional affiliations.

## Affiliations

Fisnik Aliaj<sup>1</sup>  · Naim Sylja<sup>1</sup>  · Ardita Kurtishaj<sup>1</sup> · Njomza Elezaj<sup>1</sup> · Zeqë Tolaj<sup>1</sup>  · Tahir Arbneshi<sup>2</sup>  · Arbër Zeqiraj<sup>1,3</sup> 

<sup>1</sup> Department of Physics, University of Prishtina, Eqrem Çabej Str. 51, 10000 Prishtina, Kosovo

<sup>2</sup> Department of Chemistry, University of Prishtina, Agim Ramadani Str. nn, 10000 Prishtina, Kosovo

<sup>3</sup> Department of Materials and Metallurgy, University of Mitrovica, PIM-Trepça, 40000 Mitrovica, Kosovo